Received: 19 December 2024 | Revised: 14 April 2025 | Accepted: 21 April 2025

DOI: 10.1002/alz.70347

Alzheimer's & Dementia®
THE JOURNAL OF THE ALZHEIMER'S ASSOCIATION

RESEARCH ARTICLE

Regional effects of gantenerumab on neuroimaging biomarkers in the DIAN-TU-001 trial

Austin McCullough[1] | Charles D. Chen[1] | Brian A. Gordon[1] | Nelly Joseph-Mathurin[1] | Clifford R. Jack Jr[2] | Robert Koeppe[3] | Russ Hornbeck[1] | Deborah Koudelis[1] | Nicole S. McKay[1] | Diana A. Hobbs[1] | Shaney Flores[1] | Sarah J. Keefe[1] | Neelum T. Aggarwal[4] | Ricardo F. Allegri[5] | Sarah B. Berman[6] | Thomas Bird[7] | Sandra E. Black[8] | William S. Brooks[9,10] | Jasmeer P. Chhatwal[11] | Gregory S. Day[12] | Martin R. Farlow[13] | Nick C. Fox[14] | Serge Gauthier[15] | Lawrence S. Honig[16] | Ging-Yuek Hsiung[17] | Mathias Jucker[18,19] | Johannes Levin[20,21,22] | Mario Masellis[8] | Colin Masters[23] | Patricio Chrem Mendez[5] | John M. Ringman[24] | B. Joy Snider[1] | Stephen Salloway[25,26] | Peter R. Schofield[9,10] | Hiroyuki Shimada[27] | Kazushi Suzuki[28] | Christopher H. van Dyck[29] | Gregory Klein[30] | David B. Clifford[1] | Carlos Cruchaga[1] | Jason Hassenstab[1] | Yan Li[1] | Eric McDade[1] | Susan Mills[1] | John C. Morris[1] | Richard J. Perrin[1] | Charlene Supnet-Bell[1] | Guoqiao Wang[1] | Chengjie Xiong[1] | Randall J. Bateman[1] | Tammie L. S. Benzinger[1] | for the DIAN-TU Study Team

Correspondence
Tammie L.S. Benzinger, Mallinckrodt Institute of Radiology, Washington University School of Medicine in St. Louis, Campus Box 8131, 510 South Kingshighway Boulevard, St. Louis, MO 63110, USA.
Email: benzingert@wustl.edu

Funding information
National Institute on Aging; National Institutes of Health, Grant/Award Numbers: U01AG042791, T32AG078117-01, U01AG042791-S1, R01AG046179, R01AG053267, R01AG053267-S1, R01AG053267-S2; F. Hoffman-LaRoche Ltd; Eli Lilly and Company; F. Hoffman-LaRoche Ltd.; Avid Radiopharmaceuticals; GHR

Abstract

INTRODUCTION: Monoclonal anti-amyloid therapies are now accessible, but how these treatments influence changes within the brain is still not clear. We investigated overall and regional change in amyloid removal, glucose metabolism, and atrophy in trial participants with dominantly inherited Alzheimer's disease (DIAD).

METHODS: In the DIAN-TU-001 trial, 92 carriers received gantenerumab or placebo and underwent serial neuroimaging assessments including [^{11}C]-Pittsburgh compound-B (PiB) positron emission tomography (PET), [^{18}F]-fluoro-2-deoxyglucose (FDG) PET, and magnetic resonance imaging (MRI).

RESULTS: Gantenerumab significantly reduced PiB-PET uptake overall and in most regions and showed no changes in FDG-PET or MRI measures. Drug effects were associated with baseline PiB-PET uptake, and the largest effects occurred in medial regions.

Austin McCullough, Charles D. Chen, and Brian A. Gordon contributed equally to the study.

Foundation; Cerveau Technologies, Cogstate, and Signant; NIH, Grant/Award Numbers: U01AG042791, T32AG078117-01; N.J.M., Grant/Award Numbers: 1K01AG080123, AARFD-20-681815; BrightFocus Foundation, Grant/Award Number: A2022013F; Alzheimer's Association, Grant/Award Number: AARF-21-722077

DISCUSSION: Treated DIAD participants, and especially those with higher amyloid burden, showed a decrease in PiB-PET uptake, which was more pronounced in the basal ganglia and medial frontal structures. These results may inform patient response and future drug trial design.

KEYWORDS
amyloid targeted monoclonal antibody, autosomal dominant Alzheimer's disease (ADAD), DIAN-TU, dominantly inherited Alzheimer's disease (DIAD), FDG-PET, gantenerumab, imaging outcomes, MRI measures, PET, regional PiB-PET uptake, regional variability

Highlights

- Gantenerumab unevenly decreased Aβ burden as measured by PiB-PET across brain regions.
- The strongest decrease in PiB-PET uptake was in basal ganglia and medial frontal structures.
- Variable drug effect on Aβ was partly due to the amount of burden present before treatment.
- There was no regional effect on FDG-PET metabolism or MRI volumetrics after 4 years.

1 | INTRODUCTION

Alzheimer's disease (AD) is a progressive neurodegenerative disorder with a decades-long cascade of pathological changes preceding the onset of clinical symptoms. The formation of extracellular amyloid beta (Aβ) plaques is hypothesized to initiate destructive cellular processes that culminate in widespread neuronal dysfunction and the buildup of neurofibrillary tangles (NFTs), primarily composed of hyperphosphorylated tau protein.[1,2] To date, clinical trials have focused primarily on Aβ-lowering therapies, given the prominence of Aβ early in the disease.[3–5] The primary approaches to lowering Aβ have been either the use of drugs that alter β-site amyloid precursor protein cleavage (BACE inhibitors[6–9]) or monoclonal antibody therapies that recognize monomeric (e.g., solanezumab[10,11]) or aggregated forms of Aβ (e.g., gantenerumab[12–14]). Despite initial promise, these trials mostly failed to meet their primary clinical endpoints unless amyloid was fully removed at an early stage of disease.[15,16] Possible reasons for failure include targeting the wrong protein aggregate, poor target engagement, inadequate or poorly optimized dosing, the influence of comorbidities in trial populations, and targeting individuals too late in the disease course.[17–20]

Dominantly inherited Alzheimer's disease (DIAD) is a rare form of AD caused by mutations in either the presenilin-1 (*PSEN1*), presenilin-2 (*PSEN2*), or amyloid precursor protein (*APP*) genes. In DIAD, age of symptomatic onset is heritable and highly predictable and makes DIAD a powerful model to study the pathogenesis and progression of AD.[21] Research with DIAD participants has shown that Aβ concentrations become abnormal decades before the onset of cognitive impairment and that there are sequential downstream changes in tau phosphorylation, brain metabolism, structural declines in gray and white matter, and the formation of NFTs.[22–27]

The dominantly inherited Alzheimer network (DIAN) launched an observational study of DIAD in 2008,[28,29] and the DIAN trials unit (TU) was established in 2012 as a public-private collaboration.[30–32] The first trial (DIAN-TU-001) was launched in 2012 in asymptomatic and mildly symptomatic individuals to test the monoclonal Aβ antibody gantenerumab to abrogate disease progression in patients with DIAD.[32] The trial initially had a 2-year biomarker endpoint that transitioned to a 4-year treatment trial with a cognitive endpoint. Although the trial did not meet its cognitive endpoints within its 4-year scope, the administration of gantenerumab lowered levels of cerebral Aβ measured using ^{11}C-Pittsburgh compound B (^{11}C-PiB) positron emission tomography (PET).[33] The observed longitudinal changes in volumetric estimates from MRI and brain metabolism assessed with FDG PET were not significantly different between placebo and drug arms when using the a priori defined summary measures, although significant reductions in cerebrospinal fluid (CSF) total tau and phosphorylated tau181 (p-tau181), and slowed increases in CSF neurofilament light chain (NfL) concentrations were observed in the gantenerumab group relative to placebo.[33]

Gantenerumab is a fully human monoclonal antibody that binds and removes aggregated Aβ by Fc receptor-mediated phagocytosis.[34,35] Early trials in patients with late-onset, sporadic AD found significant dose-dependent reductions in Aβ tracer uptake in participants receiving gantenerumab, assessed using florbetapir PET.[13,14] A substudy of participants enrolled in the open-label extension of these trials with titration schedules up to 1200 mg every 4 weeks showed mean Aβ reduction levels of 90.3 Centiloids in the treatment-naïve group and 57

and 74.9 Centiloids for the previously treated groups at Year 3. These reductions resulted in 80% of participants having values below the amyloid positivity threshold.[14] The initial analyses of the DIAN-TU-001 data[33] looked only at prespecified summary neuroimaging variables and did not account for regional heterogeneity. There is an urgent need to understand what impact anti-amyloid treatments have on Aβ plaques, glucose metabolism, and cortical atrophy in distinct regions of the brain to inform future drug trials and treatment plan design. Recognizing this, we aimed to assess how regional analysis of amyloid removal, glucose metabolism, and atrophy in the DIAN-TU-001 trial informed overall conclusions of 4-year gantenerumab treatment.

RESEARCH IN CONTEXT

1. **Systematic review**: The literature was reviewed using PubMed and appropriately cited trial studies of anti-amyloid immunotherapies. Gantenerumab, a monoclonal antibody targeting fibrillar Aβ, engaged its target. The primary imaging endpoint of global Aβ removal, estimated with PiB-PET, was reached in DIAD.
2. **Interpretation**: We observed regional variability in Aβ plaque removal by gantenerumab in DIAD participants. PiB-PET signal was most strongly reduced in basal ganglia and medial frontal structures, suggesting a regional susceptibility to Aβ plaque removal. For each region, this susceptibility was associated with the Aβ burden present before treatment. Removal of Aβ plaques did not influence measures of brain metabolism or cortical atrophy, suggesting the need for a longer monitoring timeframe or larger effect.
3. **Future directions**: This study demonstrates regional variability in drug effect of an anti-amyloid agent in DIAD and provides insights into the design of future clinical trials.

2 | MATERIALS AND METHODS

2.1 | Participants

All data were collected during the DIAN-TU-001 trial (trial registration number: NCT01760005). Two hundred eleven participants were referred to DIAN-TU-001 from DIAN observational (DIAN-OBS), DIAN Expanded Registry, DIAN-TU, and partner sites. Eligibility criteria included participants known to have or to be at risk of a DIAD mutation, to be between 15 years before to 10 years after the expected age of symptom onset (EYO), and to have received a Clinical Dementia Rating (CDR) of 0 (cognitively normal) or 0.5 to 1 (early symptomatic cognitive impairment).[36] Previously published demographics of this trial cohort[33] (see also Table 1) show that, although amyloid positivity was not explicitly part of the inclusion criteria, the vast majority of participants were amyloid positive at baseline due to the EYO range and mutation carrier status requirements. Participants could choose to remain blinded to their mutation status; mutation non-carriers were assigned to placebo groups. DIAD mutation carriers were randomized 3:1 to active or placebo with a minimization procedure.[31,32,37] All study participants, personnel, and sponsors were blinded to active or placebo assignment. Data from participants in the DIAN-OBS study who met the DIAN-TU inclusion criteria were used to represent natural history controls for improved estimates of the placebo group. The DIAN-OBS and DIAN-TU studies have similar monitoring protocols, including cognitive, clinical, imaging, and biomarker measures. Statistical evaluation of characteristics for all participants is provided in Table 1.

2.2 | Study design

DIAN-TU-001 was conducted at 25 sites in seven countries, from December 2012 through November 2019. Investigators are listed in the supplementary information. Cognitive outcomes were assessed every 6 months, clinical outcomes annually, and biomarkers at baseline and at Years 1, 2, and 4. A common close design ensured double-blind treatment continued for all participants until the last participant reached 4 years. Based on the results of concurrent phase 2 and 3 trials in sporadic AD,[13,14,38] target drug doses were increased approximately midway or later through the study. Gantenerumab was increased from 225 mg (subcutaneously, every 4 weeks) to 1200 mg in 2016.[33]

Some participant dropout was observed over the course of the trial (Table 2). This can be attributed mainly to (1) participant dropout due to pathology advancement and (2) data loss due to rigorous imaging quality control measures. While the modeling strategy used attempted to account for this asymmetrical dropout, its potential effects on these results must be noted.

2.3 | Imaging methods

Magnetic resonance imaging (MRI) was performed using the Alzheimer's Disease Neuroimaging Initiative protocol. T1-weighted images (1.1 × 1.1 × 1.2 mm voxels) were acquired for all participants on a 3T MRI scanner. The DIAN MRI and PET quality control (QC) cores screened images for protocol compliance, imaging artifacts, and amyloid-related imaging abnormalities.[39] Volumetric segmentation and cortical surface reconstruction were completed using FreeSurfer version 5.3 to define cortical and subcortical regions of interest (ROIs).[40,41] Segmentations and surface reconstructions were visually inspected by members of the DIAN-TU Imaging Core and edited when needed. Subcortical volumes were corrected for intracranial volume using a regression approach.[42] Cortical thicknesses and subcortical volumes were summed across hemispheres.

ROIs defined by FreeSurfer on the MRI scans were used for the regional processing of all PET data. Aβ PET imaging was performed using ^{11}C-PiB, and ^{18}F-fluorodeoxyglucose (FDG) PET imaging was utilized as a marker of brain metabolism. Scans were processed using the PET Unified Pipeline (https://github.com/ysu001/PUP) that utilizes the ROIs defined by FreeSurfer. PiB PET data from the 40- to

TABLE 1 Baseline participant characteristics.

	Active gantenerumab	Placebo
N	52	40
Age (mean ± SD, years)	46.0 ± 10.8	44.2 ± 9.6
Female, *n* (%)	21 (40)	22 (55)
APP mutation carrier, *n* (%)	6 (12)	5 (13)
PSEN1 mutation carrier, *n* (%)	43 (83)	32 (80)
PSEN2 mutation carrier, *n* (%)	3 (6)	3 (8)
APOE ε4 carrier, *n* (%)	16 (31)	13 (32)
EYO (mean ± SD, years)	−3.5 ± 7.1	−3.5 ± 7.6
CDR 0, *n* (%)	31 (60)	22 (55)
CDR 0.5, *n* (%)	15 (29)	15 (38)
CDR 1, *n* (%)	6 (12)	3 (8)
CDR-SB (mean ± SD)	1.33 ± 2.08	1.43 ± 1.87
Digit symbol (mean ± SD)	46.96 ± 20.56	46.63 ± 19.12
MMSE (mean ± SD)	27.10 ± 3.45	26.68 ± 3.97
Logical memory (mean ± SD)	9.90 ± 6.33	9.40 ± 6.45
ISLT (mean ± SD)	5.96 ± 4.04	5.80 ± 4.42
Aβ burden (mean ± SD, PiB-PET composite SUVR)	2.64 ± 1.23	2.62 ± 1.20
Aβ burden (mean ± SD, Centiloid units)	64.75 ± 51.87	63.97 ± 49.46

Abbreviations: APOE ε4, apolipoprotein E allele ε4; CDR, Clinical Dementia Rating; CDR-SB, Clinical Dementia Rating Sum of Boxes; EYO, estimated years to symptom onset; ISLT, International Shopping List Test; MMSE, Mini-Mental State Examination; PET, positron emission tomography; PiB, Pittsburgh compound B; SD, standard deviation; SUVR, standardized uptake value ratio.

TABLE 2 Longitudinal participant data totals for each neuroimaging modality.

Modality	Baseline	Year 1	Year 2	Year 4
PIB PET				
Gantenerumab	51	48 (5.8)	44 (13.7)	35 (31.3)
Placebo	40	37 (7.5)	34 (15)	26 (35)
FDG PET				
Gantenerumab	49	48 (2)	43 (12.2)	38 (22.4)
Placebo	35	35 (0)	30 (14.3)	25 (28.6)
MRI				
Gantenerumab	52	52 (0)	48 (7.7)	40 (23.1)
Placebo	40	40 (0)	36 (10)	31 (22.5)

Note: Data represents the total number of scans used for analysis in each modality at baseline, Year 1, Year 2, and Year 4, respectively. Numbers in parentheses denote the percentage of dropout relative to baseline at each time point. Dropout in this trial occurred for two main reasons: (1) advancing pathology of participants coupled with relatively high patient burden of PET imaging and (2) quality control failures during rigorous review.
Abbreviations: FDG, [^{18}F]-Fluoro-2-deoxyglucose; MRI, magnetic resonance imaging; PET, positron emission tomography.

70-min post-injection window and FDG data from the 40- to 60-min post-injection window were converted to standardized uptake value ratios (SUVRs) using cerebellar gray matter as the reference region.[43] Data were partial volume corrected using a geometric transfer matrix approach.[43,44] A composite to represent a global measure of Aβ was calculated using the averaged SUVR values in the lateral orbitofrontal, medial orbitofrontal, precuneus, rostral middle frontal, superior frontal, superior temporal, and middle temporal regions.

Voxel-wise mean SUVR images were generated by spatial normalizing participant images onto fsaverage in MNI space and calculating the arithmetic mean at each voxel for each group. The voxel-wise results were then surface-normal projected onto the atlas pial surface for visualization.

2.4 | Statistical analysis

Methods used to predetermine sample sizes and assign participants to arms were detailed in previous trial publications.[31,33] Linear Mixed Effects version 4 (Lme4) models were constructed in R version 4.1.0 using the lme4 package.[45] Model equations were structured as follows in pseudocode:

Imaging variable ≈ baseline age + sex + apoe4 + baseline CDR + drug arm + baseline EYO + time in study + (drug arm × baseline EYO) + (drug arm × time in study) + (time in study | subject)

Random subject intercepts and slopes were included to accommodate individual variation. Models were performed with an unstructured covariance matrix to account for potential dependencies in longitudinal measurements. Models were constructed for the global summary measure of Aβ as well as for regional estimates of PiB, FDG, and structural MRI. False discovery rate (FDR) correction was used for multiple comparisons correction on regional analyses, with statistical significance for all analyses set at a corrected $p < .05$. Regional analyses and brainmaps utilized the beta weight of the *drug arm × time in study* two-way interaction term from LME models to quantify the estimated longitudinal effect of gantenerumab use on imaging variables. An additional set of LME models was constructed identically except for a three-way interaction term (*drug arm × baseline EYO × time in study*) being included. This set of models was designed to test for potential changes in observed longitudinal drug effects as a function of disease state. Correlations of regional imaging variables with regional estimated drug effect beta weights were performed using a Pearson correlation.

3 | RESULTS

DIAD mutation carriers were randomized 3:1 to gantenerumab or placebo drug arms with a robust minimization procedure[37] as previously described.[31,33] This procedure minimized between-group differences at baseline in all relevant participant statistics, including genetic, cognitive, imaging, and disease state categories (Table 1). At baseline, 58% of participants were considered cognitively unimpaired

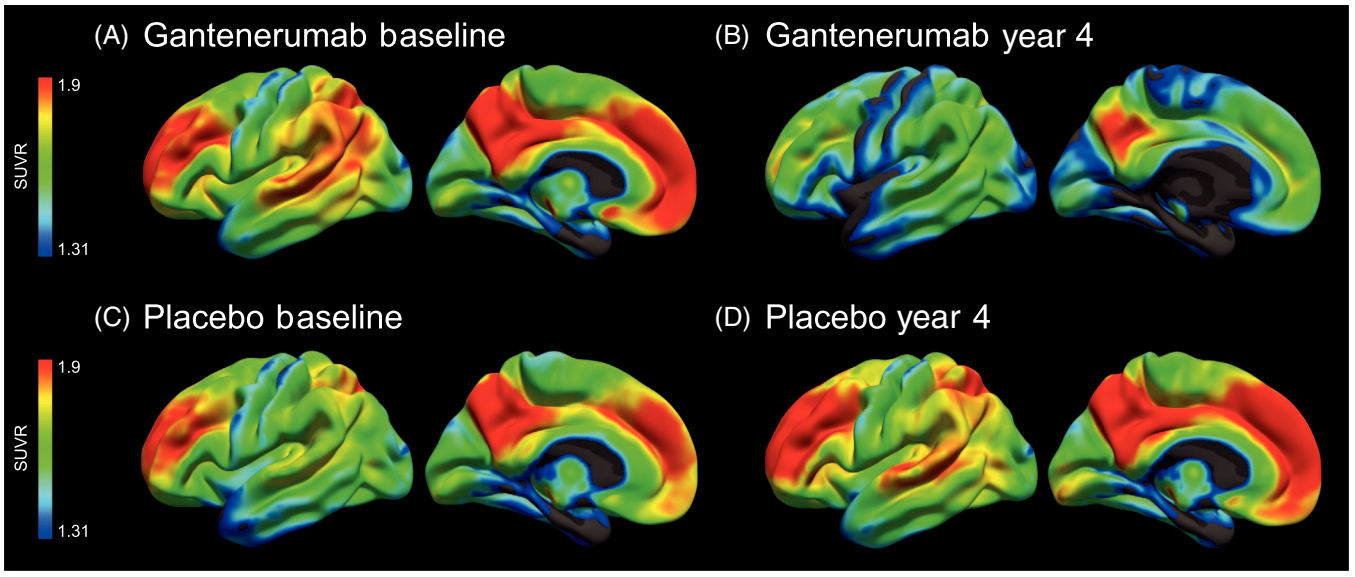

FIGURE 1 Voxel-wise mean PiB PET SUVR levels in 4-year completer participants by drug status. Voxel-wise mean PiB PET SUVR levels across the subset of participants who completed the 4-year trial course at (A) baseline (Year 0) in drug group, (B) Year 4 in drug group, (C) baseline (Year 0) in placebo group, and (D) Year 4 in placebo group. To visualize voxel-wise results, non-partial-volume-corrected data were used. PET, positron emission tomography; PiB, Pittsburgh compound B; SUVR, standardized uptake value ratio.

(CDR 0) and 42% of participants were considered cognitively impaired (CDR > 0). Baseline mean amyloid burden across the groups was 64 Centiloids, with a wide standard deviation reflecting a large within-group diversity of disease states while maintaining between-group integrity (Table 1).

Analysis on the subset of participants who completed the entire 4-year trial course resulted in a reduction of average mean cortical PiB PET signal from 2.49 SUVR (64.6 Centiloids) at baseline to 2.09 SUVR (46.6 Centiloids) at Year 4 in the gantenerumab group, as opposed to a rise from 2.27 SUVR (54.2 Centiloids) at baseline to 2.61 SUVR (70.0 Centiloids) at Year 4 in the placebo group. Figure 1 illustrates the voxel-wise cortical PiB PET SUVR values in gantenerumab and placebo groups in trial completers using non-partial-volume-corrected data.

LME model analysis on the entire trial dataset revealed that treatment with gantenerumab significantly reduced the longitudinal increase of mean cortical PiB PET signal (β = −0.15, SE = 0.026, df = 71.26, t = −5.88, $p(fdr)$ = $4.68_{10}{}^{-07}$ *[benefit is neg.]*) relative to the placebo group (Table 2). Additionally, gantenerumab treatment significantly reduced longitudinal PiB PET in 32 of 34 cortical and seven of nine subcortical regions examined (Table 3). The effect strength of gantenerumab on longitudinal PiB PET values varied considerably, with the most significant effects seen in the dorsal striatum (caudate β = −0.35, SE = 0.045, df = 77.03, t = −7.91, $p(fdr)$ = $3.39_{10}{}^{-10}$; putamen β = −0.28, SE = 0.035, df = 77.02, t = −8.04, $p(fdr)$ = $3.39_{10}{}^{-10}$), thalamus (β = −0.17, SE = 0.024, df = 82.17, t = −6.92, $p(fdr)$ = $1.31_{10}{}^{-08}$), anterior cingulate (rostral anterior cingulate β = −0.23, SE = 0.034, df = 69.47, t = −6.89, $p(fdr)$ = $1.90_{10}{}^{-08}$; caudal anterior cingulate β = −0.23, SE = 0.034, df = 69.20, t = −6.88, $p(fdr)$ = $1.90_{10}{}^{-08}$), and medial orbitofrontal (β = −0.21, SE = 0.033, df = 77.46, t = −6.34, $p(fdr)$ = 1.02_{10}-^{07}) regions (Table 3, Figures 2A and 3).

Many of the regions with high drug effects also displayed prominent baseline PiB PET signals, although posterior cortical structures with prominent baseline PiB PET signals showed noticeably smaller, but still significant, drug effects (precuneus β = −0.16, SE = 0.031, df = 70.19, t = −5.27, $p(fdr)$ = $4.00_{10}{}^{-06}$; posterior cingulate β = −0.17, SE = 0.032, df = 63.47, t = −5.26, $p(fdr)$ = $4.60_{10}{}^{-06}$; isthmus cingulate β = −0.11, SE = 0.023, df = 65.77, t = −4.75, $p(fdr)$ = $2.08_{10}{}^{-05}$) (Figures 2B and 3). Figure 3 corroborates the regional model results by showing baseline normalized end-of-trial PiB PET SUVR values for four key regions displaying a large variance in beta weight values of the drug × time model component (Figure 3). A direct correlation between regional estimated drug effect values to regional baseline estimates of pathology revealed a Pearson correlation of $r(43)$ = 0.75, p = $2_{10}{}^{-08}$, with several subcortical structures having outsized model beta weights relative to their baseline PiB PET levels (Figure 2C). No statistically significant differences between gantenerumab and placebo arms were found in the regional analyses for PiB when applying the three-way interaction (Table S1). Although biomarker changes in FDG and MRI metrics were observed over the course of the trial consistent with established yearly changes in these biomarkers at early preclinical stage of the disease,[33] no significant differences were found in any regional analysis between gantenerumab and placebo arms in FDG and MRI (Tables S2, S3a, and S3b).

4 | DISCUSSION

Top-line results from the DIAN-TU-001 trial demonstrated a significant effect of gantenerumab on global Aβ load clearance.[33] The current analyses establish that the estimated efficacy of gantenerumab was

TABLE 3 Regional LME model outputs for drug arm × time in study model component.

Region name	Component estimate (β)	Standard error	Degrees of freedom	*t* value	FDR *p* value
Summary metric models					
Mean cortical	−0.15	0.02	71.08	−5.87	**1.28E-07**
Subcortical region models					
Caudate	−0.35	0.04	77.03	−7.91	**3.39E-10**
Putamen	−0.28	0.04	77.02	−8.05	**3.39E-10**
Thalamus	−0.17	0.02	82.17	−6.92	**1.31E-08**
Nucleus accumbens	−0.28	0.05	71.78	−5.76	**6.15E-07**
Pallidum	−0.10	0.02	79.21	−4.58	**2.85E-05**
Ventral diencephalon	−0.03	0.01	85.46	−2.31	**2.65E-02**
Hippocampus	−0.01	0.01	229.06	−2.06	**4.47E-02**
Amygdala	−0.02	0.01	74.59	−1.57	1.26E-01
Brainstem	−0.01	0.01	81.00	−1.20	2.39E-01
Cortical regions models					
Rostral anterior cingulate	−0.23	0.03	69.47	−6.89	**1.90E-08**
Caudal anterior cingulate	−0.23	0.03	69.20	−6.88	**1.90E-08**
Medial orbitofrontal	−0.21	0.03	77.45	−6.34	**1.02E-07**
Paracentral	−0.18	0.03	78.56	−6.09	**2.10E-07**
Insula	−0.11	0.02	78.47	−6.07	**2.10E-07**
Parahippocampal	−0.08	0.01	77.39	−6.12	**2.10E-07**
Lateral orbitofrontal	−0.15	0.03	77.63	−5.90	**3.93E-07**
Superior frontal	−0.17	0.03	73.57	−5.80	**5.78E-07**
Superior temporal	−0.13	0.02	69.54	−5.80	**6.01E-07**
Transverse temporal	−0.18	0.03	71.57	−5.34	**3.11E-06**
Precuneus	−0.16	0.03	70.19	−5.27	**4.00E-06**
Posterior cingulate	−0.17	0.03	63.47	−5.26	**4.60E-06**
Banks of the superior temporal sulcus	−0.16	0.03	59.43	−5.25	**5.15E-06**
Pars opercularis	−0.15	0.03	66.72	−5.15	**5.68E-06**
Precentral	−0.10	0.02	78.19	−5.00	**7.51E-06**
Supramarginal	−0.13	0.03	60.01	−4.94	**1.32E-05**
Fusiform	−0.09	0.02	63.26	−4.92	**1.32E-05**
Pars orbitalis	−0.15	0.03	63.95	−4.87	**1.49E-05**
Isthmus cingulate	−0.11	0.02	65.77	−4.75	**2.08E-05**
Pars triangularis	−0.15	0.03	59.63	−4.76	**2.24E-05**
Temporal pole	−0.06	0.01	72.32	−4.58	**3.12E-05**
Superior parietal	−0.13	0.03	59.62	−4.59	**3.73E-05**
Postcentral	−0.11	0.02	65.39	−4.52	**4.07E-05**
Inferior temporal	−0.10	0.02	55.45	−4.39	**7.56E-05**
Pericalcarine	−0.13	0.03	67.16	−4.30	**8.04E-05**
Middle temporal	−0.11	0.02	57.28	−4.30	**9.38E-05**
Rostral middle frontal	−0.15	0.04	63.10	−4.21	**1.12E-04**
Caudal middle frontal	−0.12	0.03	65.76	−4.16	**1.21E-04**
Frontal pole	−0.17	0.04	56.98	−3.91	**3.13E-04**
Inferior parietal	−0.11	0.03	49.65	−3.52	**1.14E-03**
Lingual	−0.04	0.01	63.02	−2.79	**8.27E-03**
Cuneus	−0.05	0.02	48.30	−2.80	**8.41E-03**

(Continues)

TABLE 3 (Continued)

Region name	Component estimate (β)	Standard error	Degrees of freedom	*t* value	FDR *p* value
Entorhinal cortex	−0.02	0.01	65.89	−1.82	7.79E-02
Lateral occipital	−0.03	0.03	34.52	−0.96	3.42E-01

Note: Component estimates (β weights) represent the total effect of the predictor variable on longitudinal regional PiB PET signal over the trial period. Significant *p* values after false discovery rate (FDR) correction are in bold.

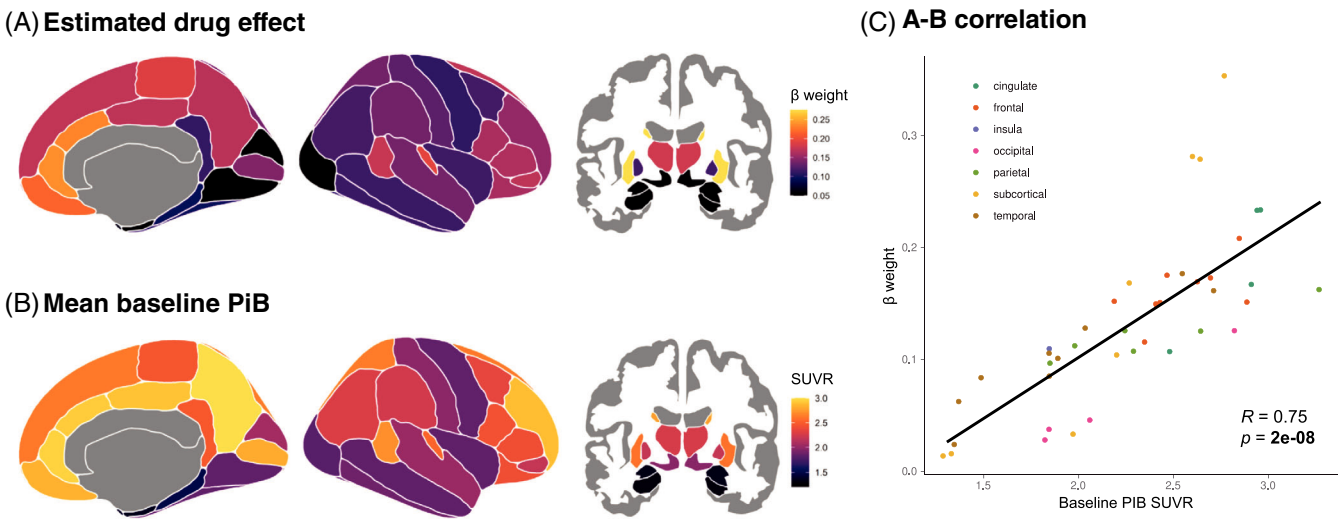

FIGURE 2 Regional differences in estimated drug effect on PiB PET signal levels. (A) Regional linear mixed-effects models were used to estimate effect of longitudinal gantenerumab use on PiB PET signal. Regional PiB PET signal was dependent variable, with fixed-effects covariates age, sex, CDR, ApoE ε4 status, and drug × time interaction term, and subject-specific random slopes and intercepts were modeled. (A) Beta weights for drug × time interaction term are displayed. (B) Regional mean baseline PiB PET signal for trial participants. (C) Pearson correlation between regional estimated drug-effect beta weights and baseline PiB PET pathology levels observed. Colors classify each region by spatial location in the brain. ApoE, apolipoprotein E; CDR, Clinical Dementia Rating; PET, positron emission tomography; PiB, Pittsburgh compound B.

not homogenous across the brain but varied by region, with the greatest effects observed in the dorsal striatum, thalamus, nucleus accumbens, caudal anterior cingulate, rostral anterior cingulate, and medial frontal regions (Table 3, Figures 2A and 3). Recognizing and understanding what drives these spatial patterns is of high interest to inform future clinical trials, as it may elucidate the way the drug is behaving in the brain.

A major contributing factor to these regional differences is the baseline level of Aβ pathology in each region prior to drug administration, as evident by the spatial similarity between the two (Figure 2A,B). However, data presented here suggest this relationship does not fully explain the regional differences in estimated drug effects (Figures 2C and 3). In both sporadic AD and DIAD, posterior parietal regions are one of the earliest regions to demonstrate Aβ deposition and reach the highest levels of pathology accumulation.[24,46] In DIAD, many participants also show substantial buildup of Aβ in the dorsal striatum, although to a lesser extent than in both parietal and medial frontal regions.[24,46,47] The current results show the greatest estimated drug effect was seen in the dorsal striatum, thalamus, nucleus accumbens, anterior cingulate, and medial frontal regions of the brain, with more modest, albeit significant, effects in posterior parietal regions (Table 3, Figure 2A). In particular, several subcortical structures showed relatively high regional model beta weights relative to their baseline amyloid pathology levels (Figure 2) and display larger average reductions in PiB PET SUVR values at end of trial relative to other regions (Figures 2 and 3). This suggests that drug effects are not solely proportional to baseline levels of amyloid pathology and are being influenced by other factors.

Given that regional differences in uptake between Aβ tracers have been documented in this cohort and that regional cortical rates of change in ^{11}C-PiB decreased more rapidly than ^{18}F-Florbetapir in both placebo and gantenerumab group,[48] it is possible that some of this relationship is due to the use of ^{11}C-PiB as the tracer of choice. However, drug effects remained highly significant across both Aβ tracers and recapitulated a very similar spatial pattern regardless of the tracer used.[48]

The observed spatial pattern may be driven by a unique feature of the DIAD cohort. Prior work has shown that Aβ accrual in the dorsal striatum is a feature of DIAD as well as Down syndrome (associated with triplication of *APP*)[47] and is present, but at much lower levels, in sporadic AD.[49,50] This could explain why these regions have some of the greatest reductions in the current analyses. However, evidence

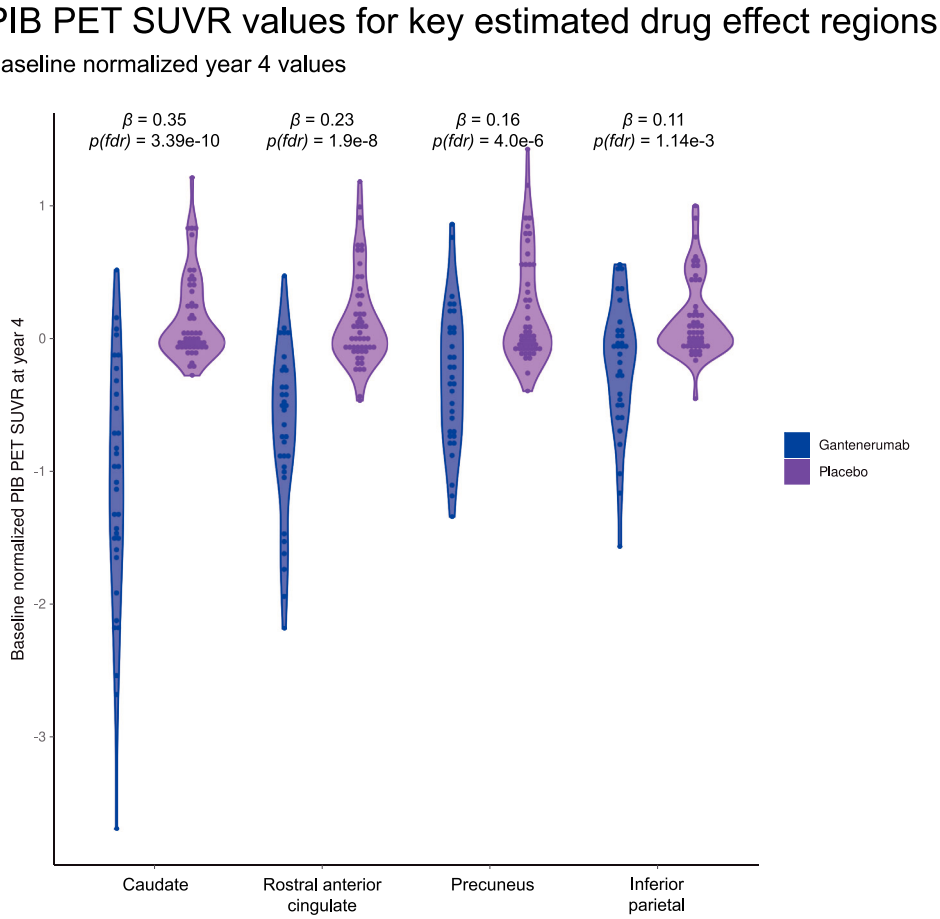

FIGURE 3 PiB PET SUVR values for key estimated drug regions. Baseline normalized PiB PET SUVR values at end of trial (Year 4) for a subcortical high estimated drug effect region (caudate), a cortical high estimated drug effect region (rostral anterior cingulate), a key region in DIAD amyloid pathology (precuneus), and a cortical region with much lower estimated drug effect results (inferior parietal) are shown to demonstrate region-specific amyloid clearance rates. Longitudinal mixed-effects model β weights and p values for each region are listed for context. PET, positron emission tomography; PiB, Pittsburgh compound B; SUVR, standardized uptake value ratio.

from previous trials in sporadic AD using gantenerumab also showed similar regional variability, with prominent regional reductions in Aβ in the dorsal striatum, anterior cingulate, and medial frontal regions.[14,38] The consistent spatial patterns suggest a common mechanism.

If the pattern is not driven by the cohort, then it is likely tied to properties of the specific regions. Previous research demonstrated that blood flow levels varied regionally across the brain,[51] and this could cause different levels of drug delivery and, therefore, pathology clearance. Additionally, it may not be overall blood flow that determines drug access, but rather blood-brain barrier (BBB) permeability.[52] Anecdotal evidence from clinical trials has shown cases where amyloid-related imaging abnormalities were associated with a corresponding local clearance of plaques interpreted as being due to increased drug accessibility.[34,53] Finally, there is evidence that lymphatic systems play a role in regulating CSF flow in the brain.[54] It may be that regional exposure to the drug is modulated by both blood flow and subsequent clearance from the brain.

Histopathological examinations have classified an array of different plaque types occurring in the brain, potentially representing different stages in the life cycle of plaque development,[55–57] and this evolution varies regionally in the brain.[58] Pharmacodynamic studies of gantenerumab show specific binding to fibrillar Aβ at sites on the N-terminal and spatially adjacent central Aβ sequences.[12,35] Thus, gantenerumab may display a different affinity, and therefore a different clearance rate, for each specific type of Aβ plaque depending upon the availability of these binding sites. Such a phenomenon may explain why medial frontal regions and basal ganglia structures displayed higher drug effects and parietal structures displayed lower estimated drug effect levels, respectively, than their baseline levels of Aβ load would suggest.

Although we found significant reduction in PiB PET signal during the 4-year trial period, we found no evidence of significant drug effects on the downstream imaging markers of FDG PET or MRI. Prior analyses of cerebrospinal fluid during the trial did reveal decreases in CSF total tau and p-tau181 levels and blunted increases in CSF NfL levels,[33] indicating at least some modification of neurodegeneration processes. This lack of effect on these imaging measures could be due to multiple causes. First, imaging measures specifically are known to be aggregate measures that include prior damage; therefore, downstream effects take a longer time to become apparent.[23–27] The 4-year

trial length, coupled with the dose escalation protocol mid-trial, meant that participants only received the highest doses of gantenerumab between Years 2 and 4.[33] Marked increases in Aβ clearance were observed during this time, suggesting that even more significant effects of gantenerumab could have been observed if higher doses had been administered throughout the trial. Second, despite significant reductions, a large majority of participants still had abnormal levels of Aβ as measured by both PiB PET signal and CSF. It may be only when levels of Aβ deposits are sufficiently reduced to normal levels or when enough bulk amyloid has been removed from the brain that neurodegenerative markers substantially improve. Additionally, the relatively low N of the trial, coupled with progressively losing some high-pathology participants due to asymmetrical dropout, could negatively affect the ability of this analysis to identify any biomarker changes beyond the strongest effects. Finally, tau PET imaging was introduced late in the trial, preventing us from relating amyloid reductions to this key marker of neurofibrillary pathology. The extension of the DIAN TU-001 into a 3-year open-label extension will address these key questions.

In conclusion, treatment with gantenerumab significantly reduced global PiB PET signal in DIAD participants over a 4-year trial period. This estimated drug effect was not ubiquitous across the brain but varied regionally, with the highest levels of signal reduction in the dorsal striatum, thalamus, nucleus accumbens, caudal anterior cingulate, rostral anterior cingulate, and medial frontal regions. Regional variations in PiB signal change were positively correlated with, but not solely explained by, levels of baseline Aβ pathology present in each region. We did not find any evidence of improvement in downstream metabolic or neurodegeneration imaging biomarkers over the 4-year trial period. These findings suggest that prolonged use of gantenerumab is effective in significantly reducing PiB PET signal, although future work is needed to evaluate whether reductions in Aβ can affect changes in clinical and neurodegenerative trajectories.

AFFILIATIONS

[1]Washington University School of Medicine in Saint Louis, St. Louis, Missouri, USA

[2]Mayo Clinic, Rochester, Minnesota, USA

[3]University of Michigan, Ann Arbor, Michigan, USA

[4]Rush University Medical Center, Chicago, Illinois, USA

[5]Institute for Neurological Research FLENI, Buenos Aires, Argentina

[6]University of Pittsburgh Medical Center, Pittsburgh, Pennsylvania, USA

[7]University of Washington, Seattle, Washington, USA

[8]Sunnybrook Health Sciences Centre, University of Toronto, Toronto, Ontario, Canada

[9]Neuroscience Research Australia, Randwick, New South Wales, Australia

[10]The University of New South Wales, UNSW Sydney, Sydney, New South Wales, Australia

[11]Massachusetts General Hospital, Brigham and Women's Hospital, Harvard Medical School, Boston, Massachusetts, USA

[12]Mayo Clinic, Jacksonville, Florida, USA

[13]Indiana University School of Medicine, Indianapolis, Indiana, USA

[14]UK Dementia Research Institute and Dementia Research Centre, UCL Queen Square Institute of Neurology, University College London, London, UK

[15]McGill Center for Studies in Aging, McGill University, Montréal, Quebec, Canada

[16]Columbia University Irving Medical Center, New York, New York, USA

[17]University of British Columbia, Vancouver, British Columbia, Canada

[18]German Center for Neurodegenerative Diseases (DZNE), Tübingen, Germany

[19]Hertie Institute for Clinical Brain Research, University of Tübingen, Tübingen, Germany

[20]German Center for Neurodegenerative Diseases (DZNE), Munich, Germany

[21]Ludwig Maximilian University of Munich, Munich, Germany

[22]Munich Cluster for Systems Neurology (SyNergy), Munich, Germany

[23]University of Melbourne, Parkville, Victoria, Australia

[24]Keck School of Medicine, University of Southern California, Los Angeles, California, USA

[25]Butler Hospital, Providence, Rhode Island, USA

[26]Warren Alpert Medical School of Brown University, Providence, Rhode Island, USA

[27]Osaka City University, Sumiyoshi-ku, Osaka, Japan

[28]National Defense Medical College, Tokorozawa, Saitama, Japan

[29]Yale School of Medicine, New Haven, Connecticut, USA

[30]Hoffmann-La Roche Ltd, Basel, Switzerland

ACKNOWLEDGMENTS

This manuscript was reviewed by DIAN-TU study investigators for scientific content and consistency of data interpretation with previous DIAN-TU study publications. We acknowledge the altruism of the participants and their families and contributions of the DIAN research and support staff at each of the participating sites for their contributions to this study. Research reported in this publication was supported by the National Institute on Aging of the National Institutes of Health under Award Numbers U01AG042791, U01AG042791-S1 (FNIH and Accelerating Medicines Partnership), R01AG046179, R01AG053267, R01AG053267-S1, R01AG053267-S2. The research for the DIAN-TU-001 gantenerumab open label extension was supported by the Alzheimer's Association and F. Hoffman-LaRoche Ltd. The research for the DIAN-TU-001 trial, solanezumab and gantenerumab drug arms, was also supported by the Alzheimer's Association, Eli Lilly and Company, F. Hoffman-LaRoche Ltd., Avid Radiopharmaceuticals (a wholly owned subsidiary of Eli Lilly and Company), GHR Foundation, an anonymous organization, Cerveau Technologies, Cogstate, and Signant. A.M. acknowledges support from the NIH (T32AG078117-01). N.J.M. acknowledges support from the NIH (1K01AG080123) and the Alzheimer's Association (AARFD-20-681815).

CONFLICT OF INTEREST STATEMENT

N.J.M. received travel support from the Alzheimer's Association to present at AAIC and an honorarium from the PeerView Institute for Medical Education for participating as a facilitator in training workshops at AAIC. C.R.J. served on a Data Safety Monitoring Board for Roche with no compensation. N.S.M. acknowledges support from BrightFocus (A2022013F) and the Alzheimer's Association (AARF-21-722077) and received honoraria from PeerView Institute for Medical Education for participating as a facilitator in training workshops

at AAIC. N.T.A. acknowledges institutional support from Eisai, Lilly, Pfizer, and Roche. R.F.A. acknowledges institutional support from the Alzheimer's Association (LatamFINGER, iLEADS) and Washington University in St. Louis. S.E.B. acknowledges institutional support from Genentech, Optina, Roche, Lilly, Eisai/Biogen Idec, NovoNordisk, Lilly Avid, ICON, Aribio Co., Ontario Brain Institute, CIHR, Leducq Foundation, Heart and Stroke Foundation of Canada, Brain Canada, Weston Brain Institute, Canadian Partnership for Stroke Recovery, Canadian Foundation for Innovation, Focused Ultrasound Foundation, Alzheimer's Association US, Queen's University, Compute Canada Resources for Research Groups, CANARIE, Networks of Centres of Excellence Canada, and received consulting fees from Roche, Biogen, NovoNordisk, Eisai, Eli Lilly, and DSR, as well as support for presentations from Biogen, Roche, and Eisai. W.S.B. received support for a presentation at Dementia Trials Australia Annual scientific meeting. J.C. received consulting fees from Humana, MedaCorp, and ExpertConnect. G.S.D. acknowledges institutional support from the NIH (R01AG089380, K23AG064029, U01NS120901, U01AG057195, U19AG032438), and received consulting fees from Parabon Nanolabs and Arialys Pharmaceuticals, support for presentations from PeerView Media, Continuing Education Inc., Eli Lilly, Ionis Pharmaceuticals, and DynaMed, personal compensation from ANI Pharmaceuticals, and material support of clinical trial (NCT04372615) from Amgen Therapeutics. M.F. received support for conduct of clinical trials from Eli Lilly, Roche/Genentech, Avanir, Biogen, Cognition Therapeutics, Green Valley, Otsuka, Neurotrope Biosciences, AZTherapies, Athira, Ionis, and Lexeo. N.C.F. received consulting fees from Eisai, Roche, Eli Lilly, and Biogen, and support for presentations from Roche. S.G. received consulting fees from AmyriAD, Eisai Canada, Enigma USA, Lilly Canada, Nordisk Canada, TauRx, and support for presentations from Otsuka Canada, and Lilly Canada. L.S.H. acknowledges institutional support from Abbvie, Acumen, Alector, AstraZeneca, Avanir, Axovant, Biogen, Bristol-Myer Squibb, Eisai, Eli Lilly, Envivo/Forum, Genentech, Janssen/Johnson & Johnson, Lundbeck, Merck, Pfizer, Roche, TauRx, Vaccinex, and received consulting fees from Biogen, Cortexyme, Eisai, Medscape, Miller Communications, and Prevail and support for presentations from Biogen, Eisai, and Medscape. G.Y.H. acknowledges institutional support from Biogen, Cassava, Eli Lilly, Eisai, NIH, and CIHR and received consulting fees from Biogen, Eli Lilly, Eisai, NovoNordisk, Roche. M.J. acknowledges institutional support from German Center for Neurodegenerative Diseases. J.L. acknowledges institutional support from German Ministry for Research and Education, Ehrmann Foundation, Lüneburg Foundation, Innovations-Fonds, Michael J. Fox Foundation, CurePSP, Jerome Lejeune Foundation, Alzheimer Forschungs Initiative, Deutsche Stiftung Down Syndrom, Else Kröner Fresenius Stiftung, DZNE MODAG GmbH, DFG (XC 2145 SyNergy – ID 390857198), and received consulting fees from Eisai, and Biogen, support for presentations from Bayer Vital, Biogen, Eisai, TEVA, Roche, Esteve, Zambon, support for attending meetings from AbbVie, and involvement in patents EP 23 156 122.6 and EP 22 159 408.8. M.M. acknowledges institutional support from Canadian Institutes of Health Research, Weston Brain Institute, Ontario Brain Institute, Brain Canada, Roche, and Alector, received consulting fees from Arkuda Therapeutics, Ionis, Alector, Wave Life Sciences, and Biogen Canada, and received support for presentations from Alcetor, Arkuda Therapeutics. J.M.R. acknowledges institutional support from the NIH (R01AG06901), Avid Pharmaceuticals, AltaMed, and CurePSP. J.S. acknowledges institutional support from the NIH, Roche, Lilly, Johnson & Johnson, and Eisai and received consulting fees from Eisai and Roche. S.S. acknowledges institutional support from Biogen, Eisai, Genentech, Roche, CognitionRx, Lilly, and Janssen, and received consulting fees from Abbvie, Acumen, Alector, Biogen, Biohaven, Cognition, Eisai, Fujirebio, Genentech, Kisbee, Labcorp, Lilly, Merck, Neurophet, NovoNordisk, Prothena, Quest, and Roche and support for meeting attendance from AbbVie, Acumen, Lilly, and Neurophet. P.R.S. acknowledges institutional support from the NIH, Anonymous Foundation, Roth Charitable Foundation, NHMRC, and MRFF and received consulting fees from Outside Opinion Pty Ltd., Moira Clay Consulting Pty Ltd., and Neuroscience Research Australia. C.H.vD. acknowledges institutional support from Lilly, Roche, Biogen, Genentech, Eisai, UCB, Cerevel, and Janssen and received consulting fees from Eisai, Roche, Ono, and Cerevel. G.K. acknowledges employment and stock incentives at F Hoffman La Roche at time of study. D.B.C. received consulting fees from Seagen and Roche and payment for services from NYU Langone Medical Center, Loughren, Loughren, & Loughren PC, Powell Gilbert LLP. C.C. acknowledges institutional support from the NIH, the Alzheimer's Association, and the Michael J. Fox Foundation and received consulting fees from Circular Genomics, Alector, and leadership and stock incentives at Vivid Genetics and Circular Genomics. J.H. received consulting fees from Prothena and AlzPath. E.M. acknowledges institutional support from the NIH (U19AG032438, U01AG059798, R13AG055232, K-award) and the Alzheimer's Association and received payment for services from Eisai, AAN, and financial incentives from C2N diagnostics. J.C.M. acknowledges institutional support from the NIH (P30 AG066444, P01AG003991, P01AG026276) and received consulting fees from Barcelona Brain Research Center, Native Alzheimer Disease-Related Resource Center in Minority Aging Research, and payment for presentations from AAIM, International Brain Health Symposium. R.J.P. acknowledges institutional support from the NIH. C.X. acknowledges institutional support from the NIH and received consulting fees from Diadem. R.J.B. acknowledges institutional support from the NIH, GHR Foundation, Alzheimer's Association, and DIAN-TU Pharma Consortium and receives financial incentives from C2N Diagnostics, support for presentations from the Korean Dementia Association, American Neurological Association, Weill Cornell Medical College, Fondazione Prada, Harvard University, University of Pennsylvania, involvement in US patents 12/267,974; 13/005,233; 62/492,718; 16/610,428; 17/015,985; 15/515,909, leadership role in C2N Diagnostics, and receipt of equipment and materials from Eisai, Janssen, and Hoffman La Roche. T.L.S.B. acknowledges institutional support from Siemens and received consulting fees from Biogen, Eli Lilly, Eisai, Bristol Myers Squibb, Johnson & Johnson, Merck, MedScape, PeerView, involvement in US patents 16/097,457; 12/016,701, and receipt of equipment and materials from Avid Radiopharmaceuticals/Eli Lilly, LMI, Lantheus, and Hyperfine. The other authors report no

conflicts of interest. Author disclosures are available in the Supporting Information.

CONSENT STATEMENT

All participants or their caregivers provided written informed consent approved by their local Institutional Review Board.

REFERENCES

1. Jack CR, Bennett DA, Blennow K, et al. NIA-AA research framework: toward a biological definition of Alzheimer's disease. *Alzheimers Dement*. 2018;14(4):535-562. doi:10.1016/j.jalz.2018.02.018
2. Braak H, Thal DR, Ghebremedhin E, Del Tredici K. Stages of the pathologic process in Alzheimer disease: age categories from 1 to 100 years. *J Neuropathol Exp Neurol*. 2011;70(11):960-969. doi:10.1097/NEN.0b013e318232a379
3. Hardy J, Selkoe DJ. The amyloid hypothesis of Alzheimer's disease: progress and problems on the road to therapeutics. *Science*. 2002;297(5580):353-356. doi:10.1126/science.1072994
4. Karran E, Mercken M, Strooper BD. The amyloid cascade hypothesis for Alzheimer's disease: an appraisal for the development of therapeutics. *Nat Rev Drug Discov*. 2011;10(9):698-712. doi:10.1038/nrd3505
5. Barage SH, Sonawane KD. Amyloid cascade hypothesis: pathogenesis and therapeutic strategies in Alzheimer's disease. *Neuropeptides*. 2015;52:1-18. doi:10.1016/j.npep.2015.06.008
6. Egan MF, Kost J, Tariot PN, et al. Randomized trial of verubecestat for mild-to-moderate Alzheimer's disease. *N Engl J Med*. 2018;378(18):1691-1703. doi:10.1056/NEJMoa1706441
7. Neumann U, Ufer M, Jacobson LH, et al. The BACE -1 inhibitor CNP 520 for prevention trials in Alzheimer's disease. *EMBO Mol Med*. 2018;10(11):e9316. doi:10.15252/emmm.201809316
8. Henley D, Raghavan N, Sperling R, Aisen P, Raman R, Romano G. Preliminary results of a trial of atabecestat in preclinical Alzheimer's disease. *N Engl J Med*. 2019;380(15):1483-1485. doi:10.1056/NEJMc1813435
9. Lo AC, Evans CD, Mancini M, et al. Phase II (NAVIGATE-AD study) results of LY3202626 effects on patients with mild Alzheimer's disease dementia. *J Alzheimers Dis Rep*. 2021;5(1):321-336. doi:10.3233/ADR-210296
10. Dodart JC, Bales KR, Gannon KS, et al. Immunization reverses memory deficits without reducing brain Aβ burden in Alzheimer's disease model. *Nat Neurosci*. 2002;5(5):452-457. doi:10.1038/nn842
11. Honig LS, Vellas B, Woodward M, et al. Trial of solanezumab for mild dementia due to Alzheimer's disease. *N Engl J Med*. 2018;378(4):321-330. doi:10.1056/NEJMoa1705971
12. Bohrmann B, Baumann K, Benz J, et al. Gantenerumab: a novel human anti-Aβ antibody demonstrates sustained cerebral amyloid-β binding and elicits cell-mediated removal of human amyloid-β. *JAD*. 2012;28(1):49-69. doi:10.3233/JAD-2011-110977
13. Ostrowitzki S, Lasser RA, Dorflinger E, et al. A phase III randomized trial of gantenerumab in prodromal Alzheimer's disease. *Alz Res Therapy*. 2017;9(1):95. doi:10.1186/s13195-017-0318-y
14. Klein G, Delmar P, Voyle N, et al. Gantenerumab reduces amyloid-β plaques in patients with prodromal to moderate Alzheimer's disease: a PET substudy interim analysis. *Alz Res Therapy*. 2019;11(1):101. doi:10.1186/s13195-019-0559-z
15. Mintun MA, Lo AC, Duggan Evans C, et al. Donanemab in early Alzheimer's disease. *N Engl J Med*. 2021;384(18):1691-1704. doi:10.1056/NEJMoa2100708
16. Van Dyck CH, Swanson CJ, Aisen P, et al. Lecanemab in early Alzheimer's disease. *N Engl J Med*. 2023;388(1):9-21. doi:10.1056/NEJMoa2212948
17. Mehta D, Jackson R, Paul G, Shi J, Sabbagh M. Why do trials for Alzheimer's disease drugs keep failing? A discontinued drug perspective for 2010-2015. *Expert Opin Investig Drugs*. 2017;26(6):735-739. doi:10.1080/13543784.2017.1323868
18. Anderson RM, Hadjichrysanthou C, Evans S, Wong MM. Why do so many clinical trials of therapies for Alzheimer's disease fail? *Lancet*. 2017;390(10110):2327-2329. doi:10.1016/S0140-6736(17)32399-1
19. Parasrampuria DA, Benet LZ, Sharma A. Why drugs fail in late stages of development: case study analyses from the last decade and recommendations. *AAPS J*. 2018;20(3):46. doi:10.1208/s12248-018-0204-y
20. Yiannopoulou KG, Anastasiou AI, Zachariou V, Pelidou SH. Reasons for failed trials of disease-modifying treatments for Alzheimer disease and their contribution in recent research. *Biomedicines*. 2019;7(4):97. doi:10.3390/biomedicines7040097
21. Rabinovici GD. Dominantly inherited Alzheimer's disease: a compass for drug development. *Nat Med*. 2021;27(7):1148-1150. doi:10.1038/s41591-021-01434-2
22. Bateman RJ, Xiong C, Benzinger TLS, et al. Clinical and biomarker changes in dominantly inherited Alzheimer's disease. *N Engl J Med*. 2012;367(9):795-804. doi:10.1056/NEJMoa1202753
23. Ryman DC, Acosta-Baena N, Aisen PS, et al. Symptom onset in autosomal dominant Alzheimer disease: a systematic review and meta-analysis. *Neurology*. 2014;83(3):253-260. doi:10.1212/WNL.0000000000000596
24. Gordon BA, Blazey TM, Su Y, et al. Spatial patterns of neuroimaging biomarker change in individuals from families with autosomal dominant Alzheimer's disease: a longitudinal study. *Lancet Neurol*. 2018;17(3):241-250. doi:10.1016/S1474-4422(18)30028-0
25. Li D, Donohue MC. Disease progression models for dominantly-inherited Alzheimer's disease. *Brain*. 2018;141(5):1244-1246. doi:10.1093/brain/awy089
26. McDade E, Wang G, Gordon BA, et al. Longitudinal cognitive and biomarker changes in dominantly inherited Alzheimer disease. *Neurology*. 2018;91(14):e1295-e1306. doi:10.1212/WNL.0000000000006277
27. Oxtoby NP, Young AL, Cash DM, et al. Data-driven models of dominantly-inherited Alzheimer's disease progression. *Brain*. 2018;141(5):1529-1544. doi:10.1093/brain/awy050
28. Bateman RJ, Aisen PS, De Strooper B, et al. Autosomal-dominant Alzheimer's disease: a review and proposal for the prevention of Alzheimer's disease. *Alzheimers Res Ther*. 2011;3(1):1. doi:10.1186/alzrt59
29. Morris JC, Aisen PS, Bateman RJ, et al. Developing an international network for Alzheimer research: the dominantly inherited alzheimer network. *Clin Investig*. 2012;2(10):975-984. doi:10.4155/cli.12.93
30. Moulder KL, Snider BJ, Mills SL, et al. Dominantly inherited Alzheimer network: facilitating research and clinical trials. *Alzheimers Res Ther*. 2013;5(5):48. doi:10.1186/alzrt213
31. Mills SM, Mallmann J, Santacruz AM, et al. Preclinical trials in autosomal dominant AD: implementation of the DIAN-TU trial. *Rev Neurol*. 2013;169(10):737-743. doi:10.1016/j.neurol.2013.07.017
32. Bateman RJ, Benzinger TL, Berry S, et al. The DIAN-TU next generation Alzheimer's prevention trial: adaptive design and disease progression model. *Alzheimers Dement*. 2017;13(1):8-19. doi:10.1016/j.jalz.2016.07.005
33. Salloway S, Farlow M, McDade E, et al. A trial of gantenerumab or solanezumab in dominantly inherited Alzheimer's disease. *Nat Med*. 2021;27(7):1187-1196. doi:10.1038/s41591-021-01369-8
34. Ostrowitzki S. Mechanism of amyloid removal in patients with Alzheimer disease treated with gantenerumab. *Arch Neurol*. 2012;69(2):198. doi:10.1001/archneurol.2011.1538

35. Novakovic D, Feligioni M, Scaccianoce S, et al. Profile of gantenerumab and its potential in the treatment of Alzheimer's disease. *Drug Des Devel Ther*. 2013;7:1359-1364. doi:10.2147/DDDT.S53401
36. Morris JC. The clinical dementia rating (CDR): current version and scoring rules. *Neurology*. 1993;43(11):2412-2414. doi:10.1212/wnl.43.11.2412-a
37. Taves DR. Minimization: a new method of assigning patients to treatment and control groups. *Clin Pharma Ther*. 1974;15(5):443-453. doi:10.1002/cpt1974155443
38. Klein G, Delmar P, Kerchner GA, et al. Thirty-six-month amyloid positron emission tomography results show continued reduction in amyloid burden with subcutaneous gantenerumab. *J Prev Alzheimer's Dis*. 2021;8(1):3-6. doi:10.14283/jpad.2020.68
39. Sperling R, Salloway S, Brooks DJ, et al. Amyloid-related imaging abnormalities in patients with Alzheimer's disease treated with bapineuzumab: a retrospective analysis. *Lancet Neurol*. 2012;11(3):241-249. doi:10.1016/S1474-4422(12)70015-7
40. Fischl B. Automatically parcellating the human cerebral cortex. *Cereb Cortex*. 2004;14(1):11-22. doi:10.1093/cercor/bhg087
41. Fischl B. FreeSurfer. *Neuroimage*. 2012;62(2):774-781. doi:10.1016/j.neuroimage.2012.01.021
42. Buckner RL, Head D, Parker J, et al. A unified approach for morphometric and functional data analysis in young, old, and demented adults using automated atlas-based head size normalization: reliability and validation against manual measurement of total intracranial volume. *Neuroimage*. 2004;23(2):724-738. doi:10.1016/j.neuroimage.2004.06.018
43. Su Y, Blazey TM, Snyder AZ, et al. Partial volume correction in quantitative amyloid imaging. *Neuroimage*. 2015;107:55-64. doi:10.1016/j.neuroimage.2014.11.058
44. Funck T, Paquette C, Evans A, Thiel A. Surface-based partial-volume correction for high-resolution PET. *Neuroimage*. 2014;102:674-687. doi:10.1016/j.neuroimage.2014.08.037
45. Bates D, Mächler M, Bolker B, Walker S. Fitting linear mixed-effects models using lme4. *J Stat Soft*. 2015;67(1):1-48. doi:10.18637/jss.v067.i01
46. Benzinger TLS, Blazey T, Jack CR, et al. Regional variability of imaging biomarkers in autosomal dominant Alzheimer's disease. *Proc Natl Acad Sci USA*. 2013;110(47):E4502-E4509. doi:10.1073/pnas.1317918110
47. Cohen AD, McDade E, Christian B, et al. Early striatal amyloid deposition distinguishes Down syndrome and autosomal dominant Alzheimer's disease from late-onset amyloid deposition. *Alzheimers Dement*. 2018;14(6):743-750. doi:10.1016/j.jalz.2018.01.002
48. Chen CD, McCullough A, Gordon B, et al. Longitudinal head-to-head comparison of 11C-PiB and 18F-florbetapir PET in a phase 2/3 clinical trial of anti-amyloid-β monoclonal antibodies in dominantly inherited Alzheimer's disease. *Eur J Nucl Med Mol Imaging*. 2023;50(9):2669-2682. doi:10.1007/s00259-023-06209-0
49. Hanseeuw BJ, Betensky RA, Mormino EC, et al. PET staging of amyloidosis using striatum. *Alzheimers Dement*. 2018;14(10):1281-1292. doi:10.1016/j.jalz.2018.04.011
50. Chen CD, Joseph-Mathurin N, Sinha N, et al. Comparing amyloid-β plaque burden with antemortem PiB PET in autosomal dominant and late-onset Alzheimer disease. *Acta Neuropathol*. 2021;142(4):689-706. doi:10.1007/s00401-021-02342-y
51. Herscovitch P, Markham J, Raichle ME. Brain blood flow measured with intravenous H2(15)O. I. Theory and error analysis. *J Nucl Med*. 1983;24(9):782-789.
52. Banks WA. Drug delivery to the brain in Alzheimer's disease: consideration of the blood–brain barrier. *Adv Drug Deliv Rev*. 2012;64(7):629-639. doi:10.1016/j.addr.2011.12.005
53. Joseph-Mathurin N, Llibre-Guerra JJ, Li Y, et al. Amyloid-related imaging abnormalities in the DIAN-TU-001 trial of gantenerumab and solanezumab: lessons from a trial in dominantly inherited Alzheimer disease. *Ann Neurol*. 2022;92(5):729-744. doi:10.1002/ana.26511
54. Iliff JJ, Wang M, Liao Y, et al. A paravascular pathway facilitates CSF flow through the brain parenchyma and the clearance of interstitial solutes, including amyloid β. *Sci Transl Med*. 2012;4(147):147ra111. doi:10.1126/scitranslmed.3003748
55. Armstrong RA. β-amyloid plaques: stages in life history or independent origin?. *Dement Geriatr Cogn Disord*. 1998;9(4):227-238. doi:10.1159/000017051
56. D'Andrea M, Nagele R. Morphologically distinct types of amyloid plaques point the way to a better understanding of Alzheimer's disease pathogenesis. *Biotech Histochem*. 2010;85(2):133-147. doi:10.3109/10520290903389445
57. Röhr D, Boon BDC, Schuler M, et al. Label-free vibrational imaging of different Aβ plaque types in Alzheimer's disease reveals sequential events in plaque development. *Acta Neuropathol Commun*. 2020;8(1):222. doi:10.1186/s40478-020-01091-5
58. Thal DR, Capetillo-Zarate E, Del Tredici K, Braak H. The development of amyloid β protein deposits in the aged brain. *Sci Aging Knowl Environ*. 2006;2006(6):re1. doi:10.1126/sageke.2006.6.re1

SUPPORTING INFORMATION

Additional supporting information can be found online in the Supporting Information section at the end of this article.

How to cite this article: McCullough A, Chen CD, Gordon BA, et al. Regional effects of gantenerumab on neuroimaging biomarkers in the DIAN-TU-001 trial. *Alzheimer's Dement*. 2025;21:e70347. https://doi.org/10.1002/alz.70347